Monthly averages of nitrous oxide and ozone for the Northern and Southern Hemisphere high latitudes: A "1-year climatology" derived from ILAS/ILAS-II observations

F. Khosrawi,[1,2] R. Müller,[3] M. H. Proffitt,[4] and H. Nakajima[5]

Received 17 June 2005; revised 13 January 2006; accepted 7 March 2006; published 9 June 2006.

[1] Correlations of ozone (O_3) and nitrous oxide (N_2O) have been suggested as a tool for validating photochemical models and as a reference for estimating high-latitude ozone loss. However, so far no analysis of ozone-tracer relations is available that provides a good temporal coverage during all months. Here we combine measurements from the Improved Limb Atmospheric Spectrometers (ILAS/ILAS-II) to derive an O_3/N_2O climatology for the high-latitude regions in the Northern and Southern Hemisphere for each month of the year, thus providing a complete seasonal cycle. ILAS and ILAS-II operated on board the Advanced Earth Observing Satellite (ADEOS/ADEOS-II), and both instruments use the solar occultation technique. ILAS operated for 8 months in 1996/1997, and ILAS-II operated for 7 months in 2003. The ILAS-II measurements cover the months that are not available from ILAS. The ILAS/ILAS-II correlations of ozone versus nitrous oxide are organized monthly in both hemispheres by partitioning these data into equal bins of altitude or potential temperature. The resulting families of curves allow separation of ozone changes due to photochemistry from those due to transport. The combined ILAS/ILAS-II data set corroborates earlier findings that the families of O_3/N_2O curves are separated and generally do not cross and further that the separation is much clearer for the potential temperature binning than for the altitude binning. The much clearer separation for the potential temperature binning is due to transport being predominantly isentropic. Thus these curves are particularly suitable for the validation of photochemical models. The seasonal cycle of O_3/N_2O distributions in the Northern and Southern Hemisphere high latitudes is found to be rather different. In the Southern Hemisphere, O_3/N_2O distributions are influenced by the strong chemical ozone loss in the Antarctic vortex and by a much longer duration of the polar vortex. In the Northern Hemisphere, diabatic descent is much more pronounced. Solely during the setup phase of the polar vortex the N_2O/O_3 distributions in the two hemispheres are rather similar.

Citation: Khosrawi, F., R. Müller, M. H. Proffitt, and H. Nakajima (2006), Monthly averages of nitrous oxide and ozone for the Northern and Southern Hemisphere high latitudes: A ''1-year climatology'' derived from ILAS/ILAS-II observations, *J. Geophys. Res.*, *111*, D11S11, doi:10.1029/2005JD006384.

1. Introduction

[2] Throughout the year ozone (O_3) is primarily produced in the tropical stratosphere with the peak production rate occurring at an altitude of ≈30 km, while the photochemical destruction of ozone is particularly pronounced at polar latitudes during late winter and early summer. Ozone changes due to dynamical processes are caused by ascent of stratospheric air in the tropical stratosphere together with descent over the Arctic and Antarctic, which results in a seasonal transport of stratospheric air from the tropics to the polar regions, the so-called Brewer Dobson circulation [*Brewer*, 1949; *Dobson*, 1956]. The strength of the ozone transport from low latitudes to the middle and high latitudes is dependent on season.

[3] The lifetime of nitrous oxide (N_2O) in the lower stratosphere is many years, decreasing with altitude to 8 months at ≈35 km [*Stanford and Ziemke*, 1991]. Therefore N_2O can be used as a tracer of transport. N_2O is exclusively produced in the troposphere and it has a photochemical sink in the middle and upper stratosphere. Thus, in the stratosphere the mean N_2O mixing ratio decreases with increasing altitude.

[1]Department of Applied Environmental Science/Department of Meteorology, Stockholm University, Stockholm, Sweden.
[2]Also at ICG-I: Stratosphere, Forschungszentrum Jülich, Jülich, Germany.
[3]ICG-I: Stratosphere, Forschungszentrum Jülich, Jülich, Germany.
[4]Proffitt Instruments Inc., Austin, Texas, USA.
[5]National Institute of Environmental Studies, Tsukuba, Japan.

0148-0227/06/2005JD006384

[4] *Proffitt et al.* [2003] developed the use of high-resolution N_2O data to examine the observed variations in the simultaneously measured O_3 through scatter plots, so called tracer-tracer correlations. Tracer-tracer correlations of long-lived trace gases and NO_y, HCl, and O_3 have been used for a long time to identify physicochemical changes from measurements taken at a particular point in time [e.g., *Kelly et al.*, 1989; *Fahey et al.*, 1990; *Proffitt et al.*, 1990; *Müller et al.*, 1996; *Tilmes et al.*, 2003b; *Sankey and Shepherd*, 2003]. In the stratosphere, compact correlations are expected between tracers for which quasi-horizontal mixing along isentropes is fast compared to their local chemical lifetime [*Plumb and Ko*, 1992]. *Sankey and Shepherd* [2003] compared correlations of various chemical species derived from the Canadian Middle Atmosphere Model (CMAM) with observations and argued that limited sampling from satellites or aircraft could possibly lead to artificially compact correlations. However, recently it has been shown by *Müller et al.* [2005] that there is no evidence for artificially compact correlations in HALOE observations of the Arctic vortex in winter 1991/92. Measurements from ILAS/ILAS-II (Improved Limb Atmospheric Spectrometer) provide a data set with a much higher spatial and temporal resolution of the polar regions than HALOE so that artificially compact correlations are unlikely to occur. Further, a compact correlation in the true sense is not considered here.

[5] The method of *Proffitt et al.* [2003] allows to consider the correlation of N_2O and O_3 in a somewhat different way. *Proffitt et al.* [2003] considered seasonal averages of N_2O and O_3 using 8 years (1989–1996) of Northern Hemisphere data measured by in situ instrumentation on the ER-2 aircraft. In a previous study [*Khosrawi et al.*, 2004] we applied the method of *Proffitt et al.* [2003] to satellite measurements from ILAS. In contrast to the study of *Proffitt et al.* [2003], who considered data of the Northern Hemisphere for 8 years, the coverage of ILAS allowed only a study of high-latitude regions and the time period was restricted to 8 months. However, due to the availability of high-altitude data (up to 70 km for O_3 and up to 50 km for N_2O), we could extend the study of *Proffitt et al.* [2003] (which was restricted to the ER-2 ascents and descents plus flight level of approximately 20 km and a few balloon flights to 30 km) from the lower stratosphere to the upper stratosphere. Further, because of the availability of Southern Hemisphere data we could extend the work of *Proffitt et al.* [2003] to the Southern Hemisphere. Owing to the good temporal coverage of the high-latitude regions by ILAS (about 14 profiles per day) monthly scatter plots instead of seasonal scatter plots could be produced as in the work of *Proffitt et al.* [2003]. Thus a more detailed analysis of the temporal development of ozone could be given.

[6] Here, we use N_2O and O_3 measured by the Improved Limb Atmospheric Spectrometers (ILAS and ILAS-II). ILAS was launched on board the Advanced Earth Observing Satellite (ADEOS) on 17 August 1996 [*Sasano et al.*, 1999; *Nakajima et al.*, 2002] while ILAS-II was launched on board ADEOS-II on 14 December 2002 [*Nakajima et al.*, 2006a]. Measurements for 8 months and 7 months, respectively, were obtained. Here, we will extend the work of *Khosrawi et al.* [2004] to the ILAS-II data. By using the ILAS-II measurements, data for the months which were not covered by ILAS, are available. Thus we produce monthly averages of nitrous oxide and ozone for the months from April to October 2003 (ILAS measured from November 1996 to June 1997). Thus the entire Antarctic vortex and the breakup of the Arctic vortex can be examined. Further, we combine the ILAS and ILAS-II data sets, thus producing a consistent data set for a complete year. This data set allows us to give a detailed analysis of the temporal development of ozone for a complete year with a high temporal resolution. Further, this data set should provide a helpful tool for validating atmospheric models.

[7] The ILAS/ILAS-II observations are particularly suitable for studies of Arctic and Antarctic ozone loss due to their high spatial and temporal resolution inside the polar vortices [*Terao et al.*, 2002; *Tilmes et al.*, 2003b]. Recently, using ILAS-II observations [*Tilmes et al.*, 2006; S. Tilmes et al., Development of tracer-tracer correlations and chemical ozone loss during the setup phase of the polar vortex, submitted to *Journal of Geophysical Research*, 2005, hereinafter referred to as Tilmes et al., submitted manuscript, 2005] calculated ozone loss during the setup phase of the Arctic and Antarctic polar vortex and for the entire Antarctic winter 2003.

2. ILAS/ILAS-II Data

[8] The ILAS and ILAS-II instruments were operated on board the Advanced Earth Observing Satellite (ADEOS and ADEOS-II) of the Japan Aerospace Exploration Agency (JAXA). The instruments were developed by the Ministry of Environment (MOE) of Japan and both use the solar occultation technique. ILAS operated continuously for an 8-month period from 30 October 1996 to 30 June 1997 [*Sasano et al.*, 1999], while ILAS-II operated continuously for a 7-month period from 2 April 2003 to 24 October 2003 [*Nakajima et al.*, 2006a]. The entire Arctic winter of 1996/1997 and the breakup of the Antarctic vortex was measured by ILAS, while ILAS-II measured the breakup of the Arctic vortex in 1996/1997 and the entire Antarctic winter of 2003.

[9] Measurements were made about fourteen times per day in the high-latitude regions of both hemispheres. During the measurement periods the latitudes from 56°N to 70°N and from 63°S to 88°S (ILAS) and between 54°N to 71°N and 64°S to 88°S (ILAS-II) were covered (see auxiliary material[1]). Eight gases were originally measured by ILAS and ILAS-II: O_3, HNO_3, NO_2, N_2O, CH_4, H_2O, CFC-11, and CFC-12. The species $ClONO_2$ and N_2O_5 have recently been added as retrieved species [*Nakajima et al.*, 2006a, 2006b]. Here, we focus on the measurements of nitrous oxide (N_2O) and ozone (O_3). Measurements of O_3 and N_2O were made in the altitude range from 10 km (or cloud top) up to 70 km and 50 km, respectively.

[10] We use ILAS version 6.1 and ILAS-II version 1.4 data. Validation studies of ILAS version 5.2 data by *Sugita et al.* [2002] and *Kanzawa et al.* [2002] show a good agreement of ozone with correlative measurements between 11 and 64 km and of nitrous oxide between 10 and 40 km. The recent ILAS version 6.1 data have been improved compared to the former version 5.2 data [*Nakajima et al.*, 2006b]. For the ILAS II data retrieval a similar technique to

[1]Auxiliary material is available at ftp://ftp.agu.org/apend/jd/2005jd006384.

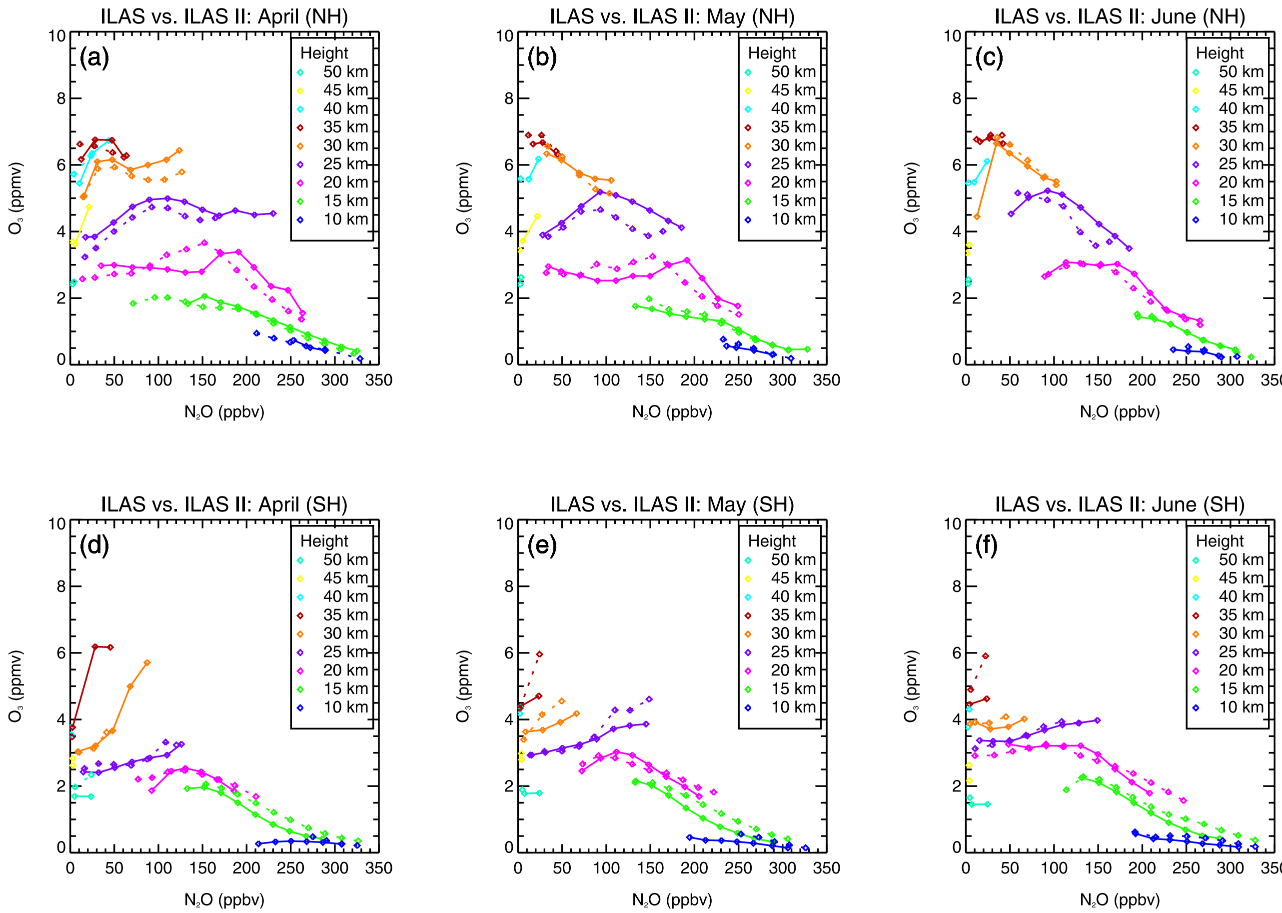

Figure 1. Monthly averaged N_2O and O_3 measured by ILAS (solid lines) and ILAS-II (dashed lines) binned by altitude (ILAS: 56°–70° (NH), 63°–88° (SH); ILAS-II: 54°–71° (NH), 64°–88° (SH)). Comparison of the months April to June for the (a–c) Northern and (d–f) Southern Hemisphere.

that of ILAS [*Yokota et al.*, 2002; T. Yokota et al., Improved Limb Atmospheric Spectrometer-II (ILAS-II) data retrieval algorithm for version 1.4 level 2 products, manuscript in preparation, 2006] was used. However, for the ILAS-II version 1.4 different data acquisition modes were used. One of the differences is the tangent height registration method (T. Tanaka et al., New tangent height registration method for the solar occultation sensor ILAS-II for data product version 1.4, manuscript in preparation, 2006). The O_3 data measured by ILAS-II are in good agreement (within ±10%) with correlative measurements between 11 and 40 km in the Northern and Southern Hemisphere [*Sugita et al.*, 2006]. However, validation studies of the ILAS-II N_2O data show a negative bias of about 10% in the Northern Hemisphere and about 20% in the Southern Hemisphere in comparison to the Odin Sub-Millimetre Radiometer (ODIN/SMR) and balloon-borne measurements (M. K. Ejiri et al., Validation of ILAS-II V1.4 nitrous oxide and methane profiles, submitted to *Journal of Geophysical Research*, 2005, hereinafter referred to as Ejiri et al., submitted manuscript, 2005). Nevertheless, this bias is not pronounced in the monthly averages of N_2O and O_3 as can be seen from the comparison of ILAS with ILAS-II (section 5.1), and therefore does not seem to have an influence on our results. The comparison of ILAS with ILAS-II served as a kind of validation for our analyses. Further, the existence of dense PSCs can cause large errors on the retrieved N_2O mixing ratios. Thereby, the estimated biases from nitric acid trihydrate (NAT) are the largest among the several types of PSCs [*Yokota et al.*, 2002, also manuscript in preparation, 2006]. These biases are not negligible since they can be as large as typical N_2O mixing ratios at 20 km in winter (Ejiri et al., submitted manuscript, 2005). Especially for ILAS version 1.4 large errors where found in the Northern Hemisphere for N_2O < 50 ppbv.

3. Method

[11] We use the method of *Proffitt et al.* [2003] and extended their analyses which is based on ER-2 measurements to satellite data [*Khosrawi et al.*, 2004]. Monthly averages of N_2O and O_3 distributions are calculated. The ILAS/ILAS-II data were organized monthly for both hemispheres by partitioning the data into equal bins of either potential temperature or altitude. The O_3 and N_2O data were then averaged within these bins over a fixed interval of N_2O (20 ppbv). The averaging of the data was performed for the levels covered by ILAS/ILAS-II (10 to 50 km and 350 to 1000 K). It should be noted here that in case of the potential temperature binning the averages reach only up to 1000 K (≈30 km) and thus not as far as the averages for the altitude binning.

[12] Monthly averages from ILAS and ILAS-II were calculated for the months April to June (the months where measurements of both instruments are available). The com-

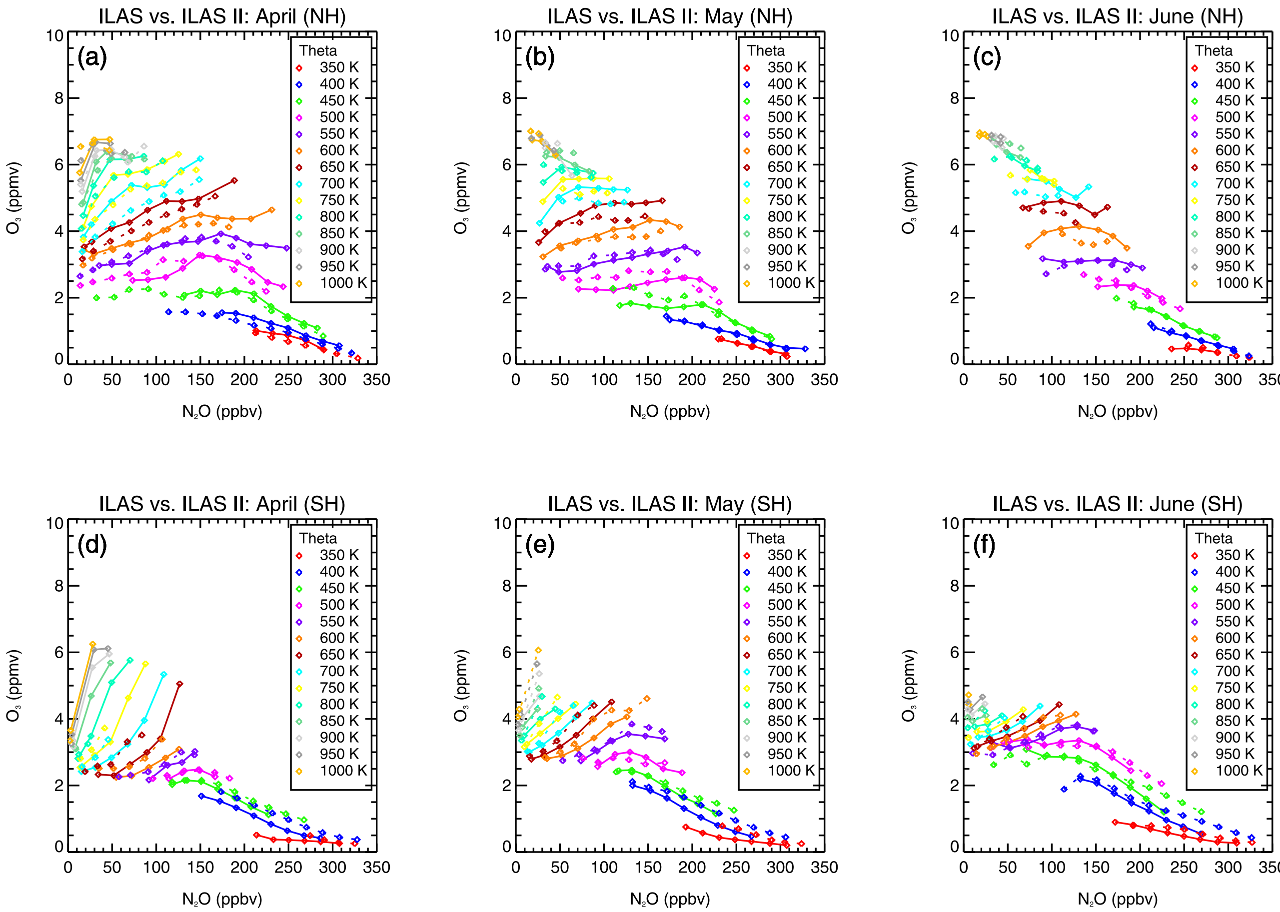

Figure 2. Monthly averaged N_2O and O_3 measured by ILAS (solid lines) and ILAS-II (dashed lines) binned by potential temperature (ILAS: 56°–70° (NH), 63°–88° (SH); ILAS-II: 54°–71° (NH), 64°–88° (SH)). Comparison of the months April to June for the (a–c) Northern and (d–f) Southern Hemisphere.

parison of the ILAS and ILAS-II data gives an overview of the general characteristics of these data sets, especially, the differences in photochemistry and dynamics between the years 1997 and 2003. Further, this comparison may serve as a kind of a validation and will give us an idea on the comparability of the data. To derive a data set for a full year, the ILAS and ILAS-II data were combined. Thus the months from January to June and November to December are covered by ILAS and the months from July to October are covered by ILAS-II. All averaged data points of the N_2O and O_3 distributions and the corresponding standard deviations are available as auxiliary material.

4. Characteristic of the N_2O/O_3 Distributions

[13] Seasonal averages of N_2O/O_3 distributions derived from ER-2 data [*Proffitt et al.*, 2003] and from ILAS data [*Khosrawi et al.*, 2004] have already been presented in previous studies. Independent of which data set is used and if monthly or seasonal averages are used the same characteristics are found in the families of curves derived from averaged N_2O and O_3 correlations.

[14] The general characteristic of the families of curves derived from the monthly averaged N_2O and O_3 correlations binned by altitude or potential temperature, is a positive correlation in the upper levels (increasing N_2O with increasing O_3) and a negative correlation in the lower levels [*Proffitt et al.*, 2003; *Khosrawi et al.*, 2004]. This change of correlation from positive to negative can be interpreted in terms of photochemical and dynamical processes. The positive correlation in the upper levels is caused by descent of air from above the O_3 maximum that brings down air that is characterized by lower O_3 and N_2O mixing ratios [e.g., *Proffitt et al.*, 2003]. Strong descent results in a steepening of the positively correlated curves (see, e.g., Figures 1d–1f). Thus the stronger the descent the stronger the steepening [*Khosrawi et al.*, 2004].

[15] Further, the curves are generally separated and do not cross. Since transport occurs mainly on isentropic levels the families of curves are much more evenly spaced for the binning by potential temperature than for the altitude binning (see, e.g., Figures 1 and 2). The good separation of these curves makes them particularly suitable for the validation of model results. The slope of the curves is further influenced by photochemical O_3 destruction [*Proffitt et al.*, 2003]. Polar winter ozone loss causes an inflection of the curves and therefore a change of slope. In summer a negative correlation (decreasing O_3 with increasing N_2O) is found at all levels since stratospheric ozone loss at high latitudes is strong [e.g., *Farman*, 1985; *Brühl and Crutzen*, 2000] and descent is weak. The summer ozone destruction tends to reduce the ozone mixing ratios and thus the

magnitude of the negative O_3/N_2O slope. Summer ozone loss from NO_x catalysis is found from May to August between ≈10 and 100 hPa in the high latitudes and in midlatitudes [*Brühl and Crutzen*, 2000]. Above 30–35 km ozone is increasingly short-lived. At these altitudes seasonal and diurnal cycles have to be taken into account.

[16] For each monthly family of curves binned by potential temperature an increase in O_3 with potential temperature (Θ) where nitrous oxide (N_2O) is held constant can be found below the O_3 maximum (≈30 km). This dependence was termed "O_3-Θ dependence" [*Proffitt et al.*, 1990, 1993, 2003] and within the Arctic vortex and below 500 K this dependence cannot be explained by descent from above the O_3 maximum. The "O_3-Θ dependence" also requires photochemical winter loss of O_3 in the presence of diabatic cooling [*Proffitt et al.*, 2003]. Although, this somewhat simplistic picture may not represent all factors affecting these families of curves in detail, it is a useful approximation.

5. Results

5.1. ILAS Versus ILAS-II

[17] The comparison between ILAS and ILAS-II helps to find differences between the years 1996/1997 and 2003, especially in the dynamics and photochemistry of the Northern Hemisphere winters of 1996/1997 and 2002/2003 at the time of the breakup of the polar vortex. In the Southern Hemisphere the formation of the polar vortex for the winter of 1997 and the entire Antarctic winter of 2003 was measured. Further, since validation studies for ILAS-II are still in progress we use the comparison of monthly averaged N_2O and O_3 from ILAS and ILAS-II as a kind of a validation to obtain an idea on the comparability of the two data sets. Furthermore, we focus on the differences between these two setup phases of the Antarctic vortex. The comparison can be used for detecting changes in the ozone distributions between the years 1997 and 2003. However, since the principal dynamical and chemical processes are the same and only the strength of these processes changes from year to year, small differences between the monthly averages derived from these two data sets are expected. Though validation studies have shown that the ILAS-II N_2O has a negative bias in comparison to the ODIN/SMR and balloon-borne measurements (Ejiri et al., submitted manuscript, 2005), this is not to pronounced in the monthly averages of N_2O and O_3 as can be seen from the following comparison. Thus it seems that the bias does not affect our results.

[18] Several studies have previously been performed investigating ozone loss in the Arctic winter of 2002/2003 [e.g., *Tilmes et al.*, 2003b, 2004; *Goutail et al.*, 2005]. *Tilmes et al.* [2004] used tracer-tracer correlations to derive chemical ozone loss for the winters of 1991–2003 using HALOE (Halogen Occultation Experiment) data. *Goutail et al.* [2005] calculated ozone loss from SAOZ measurements and REPROBUS simulations and compared their ozone loss estimates for 2002/2003 to several previous winters. In both studies a reduction in total ozone column for the winter of 2002/2003 comparable to that for the winter of 1996/1997 was found. However, in the winter of 2002/2003 the formation of PSCs, chlorine activation and thus ozone loss was already observed in early December. The breakup of the Antarctic vortex in 1996 was investigated by *Choi et al.* [2002] using ILAS methane profiles. The Antarctic winter 2003 was investigated by *Tilmes et al.* [2006, also submitted manuscript, 2005] using ILAS-II measurements. The Antarctic winter 2003 was considerably colder than the Antarctic winter in 1997. Further, ozone loss estimates derived from HALOE show that in 2003 ozone loss in the Antarctic was stronger as in 1997 (S. Tilmes et al., Arctic chemical ozone loss approaches Antarctic values, manuscript in preparation, 2006).

5.1.1. Northern Hemisphere

[19] The monthly averages of N_2O and O_3 for the months April, May and June binned by altitude (10 to 50 km with Δh = 5 km) and potential temperature (350 to 1000 K, $\Delta\Theta$ = 50 K) are shown in Figures 1a–1c and 2a–2c, respectively. In general, a good agreement can be found between ILAS and ILAS-II for the months that can be considered here. The Northern Hemisphere winter 1996/1997 and 2002/2003 were similar in their characteristic as reported by *Goutail et al.* [2005]. Model simulations by *Goutail et al.* [2005] show a reduction in total ozone column of 22% for the winter of 1996/1997 and 20% for the winter of 2002/2003. However, in the winter 2002/2003 ozone destruction started unusually early as reported by *Tilmes et al.* [2003a] based on HALOE (Halogen Occultation Experiment) observations. Already by early December, PSCs and chlorine activation was observed.

[20] In the Northern Hemispheric winter of 1996/1997 the vortex formed in November. After some disturbances in the end of November the vortex strengthened again late in December and lasted then unusually long until late in April. Until early January unusually high temperatures were found in the lower stratosphere. However, record low temperatures were reached in March and April 1997 [*Coy et al.*, 1997].

[21] In April a positive correlation is still found at the upper altitude levels (above 25 km) which changes to negative toward June at all levels (in Figures 1a–1c and 2a–2c). Photochemical ozone destruction is found at 20 ± 2.5 km (450 ± 25 and 500 ± 25 K) which is indicated by an inflection and thus a change of slope [*Proffitt et al.*, 2003]. In April a somewhat larger amount of vortex air is found in the ILAS-II data than in ILAS (air characterized by low N_2O and O_3). In May remnants of vortex air are still found in both data sets in the Northern Hemisphere. In June the curves of both data sets change their correlation to negative.

5.1.2. Southern Hemisphere

[22] The Antarctic polar vortex in the winter of 1997 started to develop in March 1997 at altitudes above 600 K and a continuous vortex was established in mid May at altitudes between 475 and 600 K (Tilmes et al., submitted manuscript, 2005). In 2003 the Antarctic polar vortex started developing at the beginning of March but was not fully established until June (Tilmes et al., submitted manuscript, 2005). Estimates of ozone loss derived from HALOE show that in the Antarctic winter 2003 ozone loss was stronger and the winter was considerably colder as in 1997 (S. Tilmes et al., Arctic chemical ozone loss approaches Antarctic values, manuscript in preparation, 2006).

[23] In the Southern Hemisphere a good agreement between ILAS and ILAS-II is also found (Figures 1d–1f and 2d–2f). While the levels above 20 km (above 550 K) are

positively correlated, the levels below are negatively correlated. However, in April in the ILAS data a stronger descent and thus a strong positive correlation is found at the levels above 25 km indicating that descent was stronger in April 1997 than April 2003. In May and June the slopes of the positively correlated curves are not as steep as in April, but the proportion between positively and negatively correlated curves is the same [*Khosrawi et al.*, 2004].

5.2. ILAS/ILAS-II: A "1-Year Climatology"

[24] In the following the combined ILAS/ILAS-II data set is used to derive a 1-year climatology for high latitudes. The ILAS/ILAS-II data are partitioned into bins of altitude and potential temperature for the Northern and Southern Hemisphere for January to December. The months from January to May and November and December are covered by the ILAS data while the months July to October are covered by the ILAS-II data.

[25] The resulting families of N_2O/O_3 curves after binning by altitude (10 to 50 km with $\Delta h = 5$ km) and after binning by potential temperature (350 K to 1000 K with $\Delta\Theta = 50$ K) are shown for the Northern Hemisphere in Figures 3 and 4 and for the Southern Hemisphere in Figures 5 and 6 (these figures including standard deviations as well as all data shown in these figures are available as auxiliary material). In the ILAS/ILAS-II data in the fall and winter months, in both hemispheres, a negative correlation of N_2O and O_3 is found for altitudes below 25 km while the curves at the levels above are positively correlated. In the curves binned by potential temperature, in all seasons, except summer, a positive correlation is found at the levels above 500 K and a negative or flat correlation in the levels below. Since transport occurs mainly on isentropic levels the curves are more clearly separated for the potential temperature binning than for the altitude binning. In Summer when at high-latitude ozone loss is strong and descent is weak a negative correlation can be found at all altitudes and a negative to flat correlation at all potential temperature levels.

5.2.1. Northern Hemisphere

[26] From January to March (Figures 3a–3c) a positive correlation is found at altitude levels above 20 km. The lower levels are negatively correlated and at 20 ± 2.5 and 25 ± 2.5 km ongoing ozone destruction is noticeable by a gradual change of slope from negatively to positive correlated [*Proffitt et al.*, 2003]. In January at 20 ± 2.5 km the inflection is found at 150 ppbv N_2O while in March the inflection is found at 190 ppbv N_2O (3 a and c). In the curves binned by potential temperature a gradual change of slope from positive to negative is noticeable along particular isentropes from January onward (Figure 4a). A positive correlation is found in the upper levels (above 500 K). At 500 K enhanced photochemical O_3 destruction causes a change of slope with an inflection at a N_2O mixing ratio of 150 ppbv. Evidence for chlorine-catalyzed photochemical O_3 destruction during this time period (late winter, early spring 1997) in the lower stratosphere was reported in previous studies based on model results and observations [e.g., *Pierce et al.*, 1997; *McKenna et al.*, 2002; *Tilmes et al.*, 2003b].

[27] In April and May, after the breakup of the polar vortex, remnants of vortex air (low O_3 and low N_2O) are found at 20 ± 2.5 and 25 ± 2.5 km (Figures 3d–3e) with an inflection at 200 ppbv N_2O and at 170 ppbv N_2O and 90 ppbv N_2O, respectively. Toward May (Figure 3e) descent is decreasing in strength and the correlation in upper levels changes to negatively correlated. In June a negative correlation is found at all levels due to weak descent though at 20 ± 2.5 km remnants of vortex air are still found. These vortex remnants are also found in the curves binned by potential temperature (450–550 K) at low N_2O values (Figure 4f). By July the remnants of the vortex air are completely mixed with the outside air, and the low O_3 and N_2O mixing ratios which were found at altitudes between 20 and 25 km (450 to 550 K) have disappeared due to the dilution with midlatitude air (Figure 3g). The N_2O/O_3 families of curves remain negatively correlated at all altitude levels during July and August. A flat or negative correlation is found at all potential temperature levels for June and July (Figures 4f–4g). Summer ozone loss due to NO_x catalyzed O_3 loss cycles [e.g., *Crutzen and Brühl*, 2001] is noticeable during that time by a general decline of ozone at altitudes above 20 km (550 K).

[28] In the families of curves binned by potential temperature descent appears as decreased ozone in July at the uppermost potential temperature levels, which continues gradually through October down to 700 K. In November and December descent continues with comparable strength. With the beginning of fall, starting in September (Figure 3i) a slope change from negatively to positively correlated is found at altitude levels above 20 km, which increases until December, thus leading to a positive correlation in the upper levels and a negative correlation in the lower levels from October to December. The positive correlation in the upper levels (20–35 km) indicates that descent of air from above the O_3 maximum which brings down air characterized by low O_3 and N_2O, has intensified [*Proffitt et al.*, 2003; *Khosrawi et al.*, 2004].

5.2.2. Southern Hemisphere

[29] In the Southern Hemisphere from January to March (Figures 5a–5c) summer ozone loss [e.g., *Johnston*, 1975; *Farman*, 1985] is noticeable by a general decline of ozone at altitudes above 20 km (550 K). In the ILAS/ILAS-II data a negative correlation is found at all altitude levels (Figures 5a–5c) from January to March. The families of curves binned by potential temperature show a flat correlation at all potential temperatures levels in January (Figure 6a). With the beginning of the formation of the polar vortex in April and the associated diabatic descent in the polar vortex region the curves exhibit a steep slope with a positive correlation at the upper altitude/potential temperature levels and a negative correlation at lower levels (Figures 5d and 6d). However, in April ozone mixing ratios are generally low due to preceding summer ozone destruction.

[30] Evidence for a strong descent motion in the Southern Hemisphere polar vortex was reported by, e.g., *Russell et al.* [1993] based on HALOE observations and descent rates have been calculated by, e.g., *Schoeberl et al.* [1995]. Recently, descent inside the Southern Hemisphere polar vortex was investigated for the early winter 1997 by *Kawamoto et al.* [2004] using ILAS N_2O and CH_4 data showing a clear downward motion from February to June with a average descent rate of 2.1 to 1.7 km per month in the middle stratosphere. In August and September ILAS-II measured close to the south pole and less pronounced

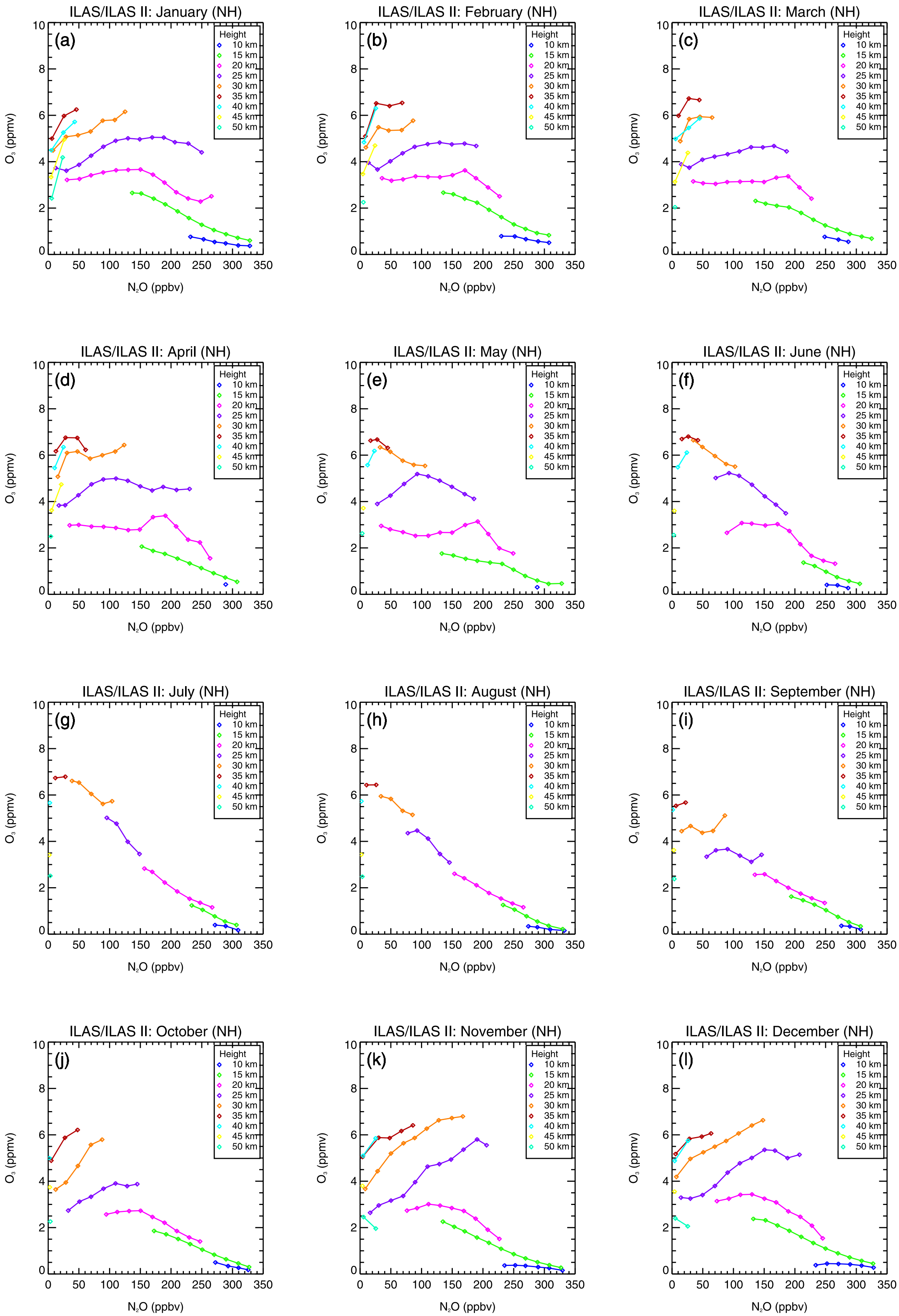

Figure 3. One-year climatology: Northern Hemispheric monthly averaged N_2O and O_3 measured by ILAS/ILAS-II binned by altitude (ILAS: 56°–70°; ILAS-II: 54°–71°). (a–f) January to June: ILAS, (g–j) July to October: ILAS-II, and (k and l) November-December: ILAS. Standard deviations are generally around 5–6 ppbv N_2O and 0.1–0.5 ppmv O_3.

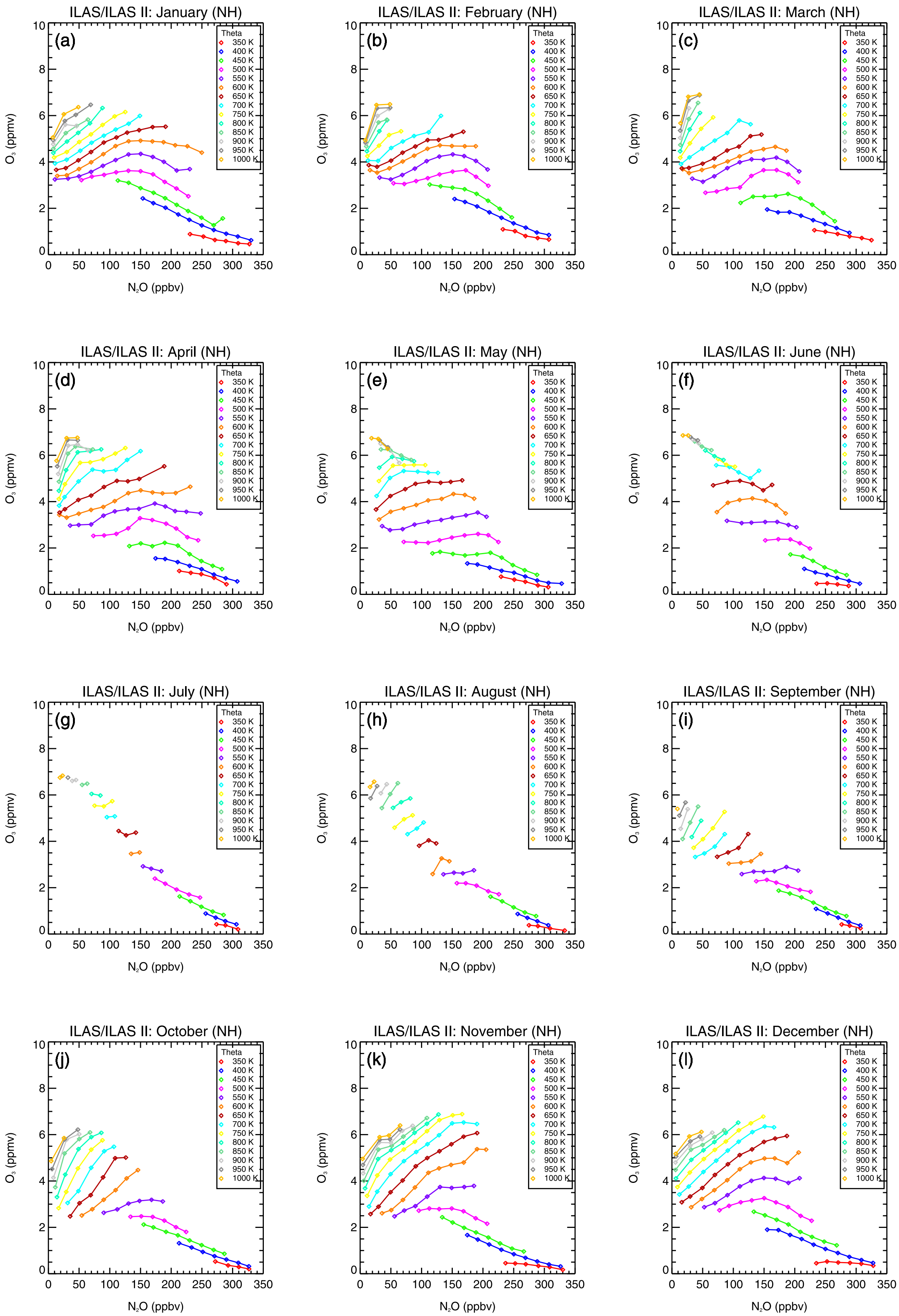

Figure 4. One-year climatology: Northern Hemispheric monthly averaged N_2O and O_3 measured by ILAS/ILAS-II binned by potential temperature (ILAS: 56°–70°; ILAS-II: 54°–71°). (a–f) January to June: ILAS, (g–j) July to October: ILAS-II, and (k and l) November–December: ILAS. Standard deviations are generally around 4–6 ppbv N_2O and 0.1–0.5 ppmv O_3.

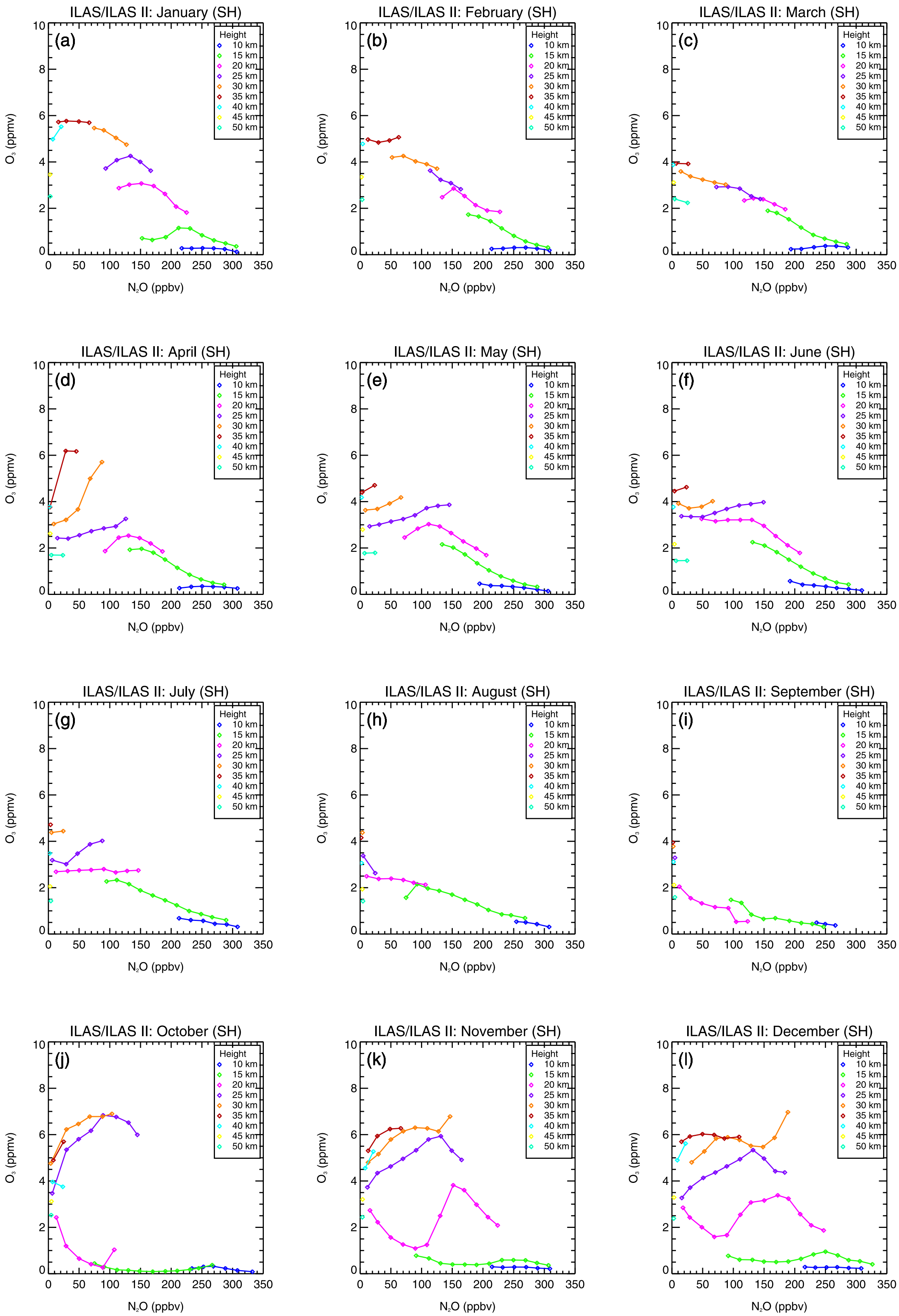

Figure 5. One-year climatology: Southern Hemispheric monthly averaged N_2O and O_3 measured by ILAS/ILAS-II binned by altitude (ILAS: 63°–88°; ILAS-II: 64°–88°). (a–f) January to June: ILAS, (g–j) July to October: ILAS-II, and (k and l) November–December: ILAS. Standard deviations are generally around 5–6 ppbv N_2O and 0.1–0.3 ppmv O_3.

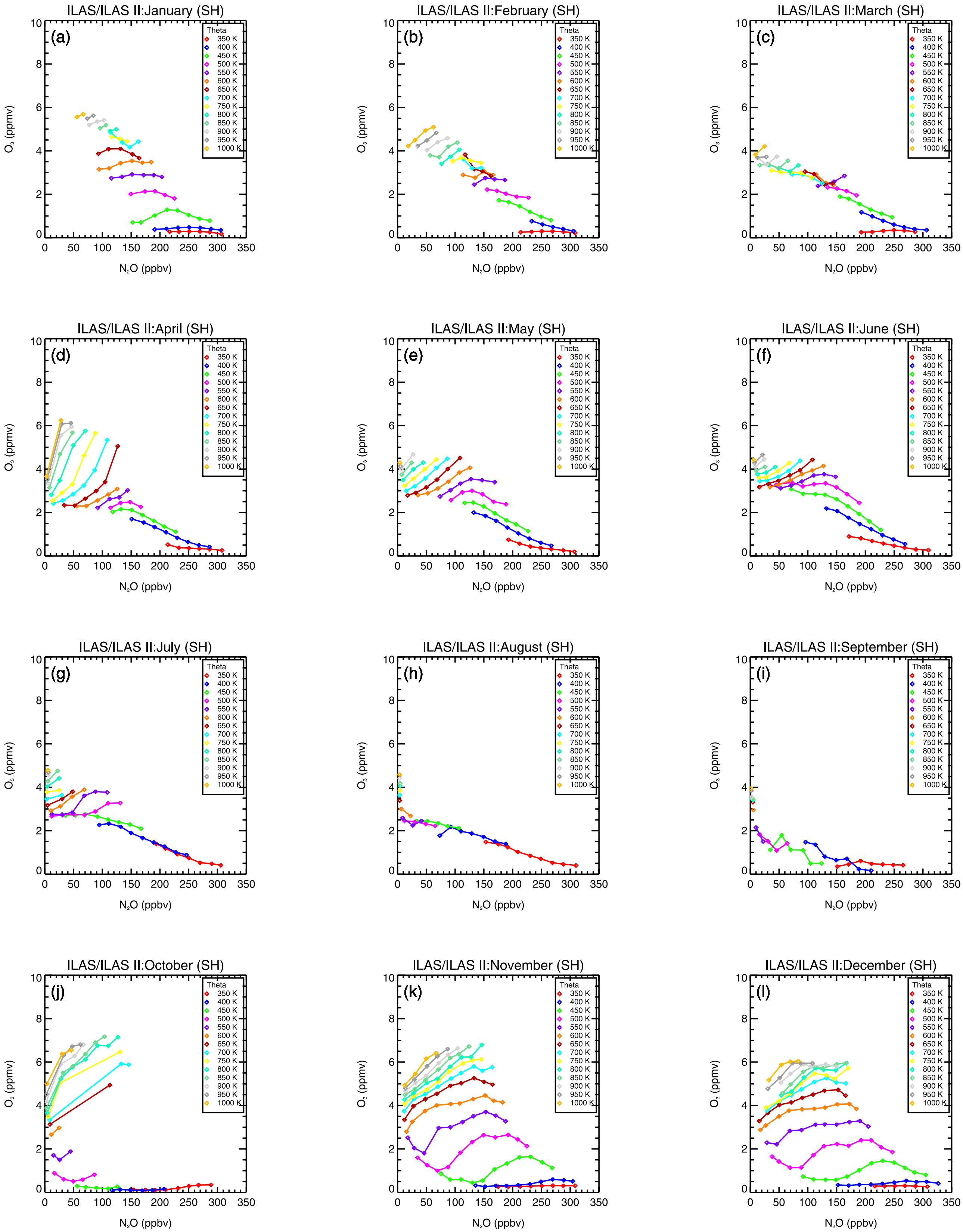

Figure 6. One-year climatology: Southern Hemispheric monthly averaged N_2O and O_3 measured by ILAS/ILAS-II binned by potential temperature (ILAS: 63°–88°; ILAS-II: 64°–88°). (a–f) January to June: ILAS, (g–j) July to October: ILAS-II, and (k and l) November–December: ILAS. Standard deviations are generally around 4–6 ppbv N_2O and 0.1–0.3 ppmv O_3.

descent is found in the data (Figures 5h, 5i, 6h, and 6i). Between May and October descent is strongest at the edge of the vortex [*Rosenfield et al.*, 1994].

[31] From May to July the levels below 450 K remain almost unchanged while in the levels above descent becomes less pronounced (Figures 6e–6g). Beginning in July polar winter ozone loss is evident in the families of curves binned by altitude and potential temperature by an inflection and thus a change of slope [*Proffitt et al.*, 2003]. In the 15 ± 2.5 km and 20 ± 2.5 km curve very low ozone values are observed from October to December (Figures 5j–5l). Due to prior ozone destruction the lowest ozone values are found in October at 15 ± 2.5 km with O_3 values almost approaching zero and at 20 ± 2.5 km with an inflection at 130 ppbv N_2O and a minimum in O_3 of 0.05 ppmv at 10 to 90 ppbv N_2O. In November the inflection in the 20 ± 2.5 km curve is found at 150 ppbv with a minimum in O_3 of 1 ppmv at 70 to 110 ppbv N_2O and in December at 190 ppbv N_2O with a minimum in O_3 of 1.5 ppmv at 70 to 90 ppbv N_2O. Very low ozone values are evident in the curves binned by potential temperature in October at 500 K with a minimum in ozone of 1 ppmv at 50 ppbv N_2O (Figure 6j). The minima of O_3 remain in November and December but with higher O_3 mixing ratios than in October.

5.2.3. Seasonal Cycle of Ozone in the Arctic and Antarctic in Comparison

[32] The combined ILAS/ILAS-II climatology allows the seasonal cycle of ozone in the Arctic and Antarctic to be compared (Figures 3 and 5 and Figures 4 and 6, respectively). The most obvious difference is the signature of the Antarctic ozone hole, that is noticeable by much lower ozone mixing ratios below 25 km (below 550 K) for the Southern Hemisphere in September and October than in March and April in the Northern Hemisphere.

[33] Further, the impact of the Antarctic vortex on the O_3/N_2O distribution may be seen as reduced values of ozone and an extension of the O_3/N_2O distribution to lower N_2O mixing ratios through November and December, whereas, in the Northern Hemisphere, in the corresponding season (May and June) no influence of the dissipating Arctic vortex is visible.

[34] Moreover, an important difference between the N_2O and O_3 distributions in the corresponding season is that diabatic descent, noticeable as a positive O_3/N_2O distribution at altitudes above 25 km (500 K), is much more pronounced in the Northern Hemisphere than in the Southern Hemisphere [e.g., *Shepherd*, 2003]. Comparable O_3/N_2O distributions for the Arctic and the Antarctic are only found during the setup phase of the polar vortex. The O_3/N_2O distribution for October in the Northern Hemisphere and April in the Southern Hemisphere are rather comparable.

6. Conclusions

[35] We use the method of *Proffitt et al.* [2003] who used averages of N_2O and O_3 to reduce the O_3 variability caused by transport processes, thereby separating photochemical contributions from dynamical. Here, we extended our previous study [*Khosrawi et al.*, 2004] where we used 8 months of ILAS data, by using ILAS-II data and combining both data sets. Though ILAS-II measured only for a period of 7 months we could investigate the temporal development of ozone through all seasons since the months which were not covered by ILAS are available from ILAS-II. This allowed us to investigate ozone changes during the time of the breakup of the Arctic vortex 2002/2003 as well as during the entire Antarctic vortex 2003.

[36] The data were binned by either altitude or potential temperature, and then averaged. The results presented here corroborate earlier findings by *Proffitt et al.* [2003] and *Khosrawi et al.* [2004] that in both hemispheres the resulting curves are separated and generally do not cross and further that the curves are better separated for the binning by potential temperature than for the binning by altitude. Except in summer, a positive O_3/N_2O correlation is found above 500 K and a negative correlation below. The positive correlation is caused by descent of air from above the O_3 maximum. That is, strong diabatic descent causes a steepening of the positively correlated curves [*Khosrawi et al.*, 2004]. Chemical ozone loss causes an inflection and thus a change of slope. Thus the slope changes with season and is not solely influenced by the intensity of descent but also by O_3 photochemistry.

[37] The development of the O_3/N_2O distribution in the Northern Hemisphere and the Southern Hemisphere over comparable seasons reveals pronounced differences. Clearly noticeable is, as expected, the strong ozone depletion in the Antarctic vortex in September and October. Further, due to the longer duration of the vortex in the Southern Hemisphere the influence of the vortex on the O_3/N_2O distribution is noticeable for much longer than in the corresponding Northern Hemisphere season.

[38] The comparison of ILAS with ILAS-II for the months where both instruments measured show a good agreement between both data sets. Further, the comparison served as a kind of validation and helped us finding differences of the ozone distribution between the years 1997 and 2003. Though ILAS-II N_2O has a negative bias compared to ODIN/SMR data (Ejiri et al., submitted manuscript, 2005) of 10% in the Northern Hemisphere and of 20% in the Southern Hemisphere this does not have an impact on our results using monthly averages of N_2O and O_3. By combining the ILAS/ILAS-II data set, we derived a 1-year climatology of O_3 and N_2O for the high latitudes. Therefore we derived a data set which may be helpful for testing and validating photochemical models and may be employed for tracking future changes of ozone in the Northern and Southern Hemispheric lower and upper stratosphere at high latitudes.

[39] **Acknowledgments.** The Improved Limb Atmospheric Spectrometers (ILAS and ILAS-II) were developed by the Ministry of the Environment of Japan. The ILAS and ILAS-II data were processed at the ILAS/ILAS-II Data Handling Facility, National Institute of Environmental Studies (NIES), Japan. A part of this work was supported by the Global Environment Research Fund provided by the Ministry of the Environment of Japan (MOE). We would like to thank T. Shepherd and D. Sankey for helpful comments on the manuscript. We also like to thank the European Commission for funding F. Khosrawi by the EU 6th Framework Programme–Marie-Curie Intra-European Fellowships.

References

Brewer, A. W. (1949), Evidence for a world circulation provided by the measurements of helium and water vapor distribution in the stratosphere, *Q. J. R. Meteorol. Soc.*, *75*, 351–363.

Brühl, C., and P. J. Crutzen (2000), NO_x-catalyzed ozone destruction and NO_x activation at midlatitudes to high latitudes as the main cause of the spring to fall stratospheric ozone decline in the Northern Hemisphere, *J. Geophys. Res.*, *105*(D10), 12,163–12,168.

Choi, W., S. Kim, W. B. Grant, M. Shiotani, Y. Sasano, and M. R. Schoberl (2002), Transport of methane in the stratosphere associated with the breakdown of the Antarctic polar vortex, *J. Geophys. Res.*, *107*(D24), 8209, doi:10.1029/2001JD000644.

Coy, L., E. Nash, and P. Newman (1997), Meteorology of the polar vortex: Spring 1997, *Geophys. Res. Lett.*, *24*, 2693–2696.

Crutzen, P. J., and C. Brühl (2001), Catalysis by NOx as the main cause of the spring to fall stratospheric ozone decline in the Northern Hemisphere, *J. Phys. Chem. A*, *105*, 1579–1582.

Dobson, G. M. B. (1956), Origin and distribution of polyatomic molecules in the atmosphere, *Proc. R. Soc. London, Ser. A*, *236*, 187–193.

Fahey, D. W., K. K. Kelly, S. R. Kawa, A. F. Tuck, M. Loewenstein, K. R. Chan, and L. E. Heid (1990), Observations of denitrification and dehydration in the winter polar stratosphere, *Nature*, *344*, 321–324.

Farman, J. C. (1985), Ozone photochemistry in the Antarctic stratosphere in summer, *Q. J. R. Meteorol. Soc.*, *111*, 1013–1025.

Goutail, F., et al. (2005), Early unusual ozone loss during the Arctic winter 2003/2003 compared to other winters, *Atmos. Chem. Phys.*, *5*, 665–677.

Johnston, H. S. (1975), Global ozone balance in the natural stratosphere, *Rev. Geophys.*, *13*, 637–649.

Kanzawa, H., et al. (2002), Validation and data characteristics of water vapor profiles observed by the Improved Limb Atmospheric Spectrometer (ILAS) and processed with the version 5.20 algorithm, *J. Geophys. Res.*, *107*(D24), 8217, doi:10.1029/2001JD000881. (Correction, *J. Geophys. Res.*, *108*(D4), 8218, doi:10.1029/20003JD001601, 2003.)

Kawamoto, N., H. Kanzawa, and M. Shiotani (2004), Time variations of descent in the Antarctic vortex during the early winter of 1997, *J. Geophys. Res.*, *109*, D18309, doi:10.1029/2004JD004650.

Kelly, K. K., et al. (1989), Dehydration in the lower Antarctic stratosphere during late winter and early spring, 1987, *J. Geophys. Res.*, *94*, 11,317–11,357.

Khosrawi, F., R. Müller, M. H. Proffitt, and H. Nakajima (2004), Monthly averaged ozone and nitrous oxide from the Improved Limb Atmospheric Spectrometer (ILAS) in the Northern and Southern Hemisphere polar regions, *J. Geophys. Res.*, *109*, D10301, doi:10.1029/2003JD004365.

McKenna, D. S., J.-U. Grooß, G. Günther, P. Konopka, R. Müller, G. Carver, and Y. Sasano (2002), A new Chemical Lagrangian Model of the Stratosphere (CLaMS): 2. Formulation of chemistry-scheme and initialization, *J. Geophys. Res.*, *107*(D15), 4256, doi:10.1029/2000JD000113.

Müller, R., P. J. Crutzen, J.-U. Grooß, C. Brühl, J. M. Russel III, and A. F. Tuck (1996), Chlorine activation and ozone depletion in the Arctic vortex: Observations by the Halogen Occultation Experiment on the Upper Atmosphere Research Satellite, *J. Geophys. Res.*, *101*, 12,531–12,554.

Müller, R., S. Tilmes, P. Konopka, J.-U. Grooß, and H.-J. Jost (2005), Impact of mixing and chemical change on ozone-tracer relations in the polar vortex, *Atmos. Chem. Phys.*, *5*, 3139–3151.

Nakajima, H., et al. (2002), Characteristics and performance of the Improved Limb Atmospheric Spectrometer (ILAS) in orbit, *J. Geophys. Res.*, *107*(D24), 8213, doi:10.1029/2001JD001439.

Nakajima, H., et al. (2006a), Characteristics and performance of the Improved Limb Atmospheric Spectrometer-II (ILAS-II) on board the ADEOS-II satellite, *J. Geophys. Res.*, *111*, D11S01, doi:10.1029/2005JD006334.

Nakajima, H., et al. (2006b), Measurements of $ClONO_2$ by the Improved Limb Atmospheric Spectrometer (ILAS) in high-latitude stratosphere: New products using version 6.1 data processing algorithm, *J. Geophys. Res.*, *111*, D11S09, doi:10.1029/2005JD006441.

Pierce, R. B., T. D. Fairlie, E. E. Remsberg, J. M. Russell, and W. L. Grose (1997), HALOE observations of the Arctic vortex during the 1997 spring: Horizontal structure in the lower stratosphere, *Geophys. Res. Lett.*, *24*, 2701–2704.

Plumb, R. A., and M. K. W. Ko (1992), Interrelationships between mixing ratios of long-lived stratospheric constituents, *J. Geophys. Res.*, *97*, 10,145–10,156.

Proffitt, M. H., J. J. Margitan, K. K. Kelly, M. Loewenstein, J. R. Podolske, and K. R. Chan (1990), Ozone loss in the Arctic polar vortex inferred from high altitude aircraft measurements, *Nature*, *347*, 31–36.

Proffitt, M. H., K. Aikin, J. J. Margitan, M. Loewenstein, J. R. Podolske, A. Weaver, K. R. Chan, H. Fast, and J. W. Elkins (1993), Ozone loss inside the northern polar vortex during the 1991–1992 winter, *Science*, *261*, 1150–1154.

Proffitt, M. H., K. Aikin, A. F. Tuck, J. J. Margitan, C. R. Webster, G. C. Toon, and J. W. Elkins (2003), Seasonally averaged ozone and nitrous oxide in the Northern Hemisphere lower stratosphere, *J. Geophys. Res.*, *108*(D3), 4110, doi:10.1029/2002JD002657.

Rosenfield, J. E., P. A. Newman, and M. R. Schoeberl (1994), Computations of diabatic descent in the stratospheric polar vortex, *J. Geophys. Res.*, *99*(D8), 16,677–16,689.

Russell, J. M., L. L. Gordley, J. H. Park, S. R. Drayson, A. F. Tuck, J. E. Harries, R. J. Cicerone, P. J. Crutzen, and J. E. Frederick (1993), The Halogen Occultation Experiment, *J. Geophys. Res.*, *98*, 10,777–10,797.

Sankey, D., and T. G. Shepherd (2003), Correlation of long-lived chemical species in a middle atmosphere general circulation model, *J. Geophys. Res.*, *108*(D16), 4494, doi:10.1029/2002JD002799.

Sasano, Y., M. Suzuki, T. Yokota, and H. Kanzawa (1999), Improved Limb Atmospheric Spectrometer (ILAS) for stratospheric ozone layer measurements by solar occultation technique, *Geophys. Res. Lett.*, *26*, 197–200.

Schoeberl, M. R., M. Luo, and J. E. Rosenfield (1995), An analyses of the Antarctic Halogen Occultation Experiment trace gas observations, *J. Geophys. Res.*, *100*, 5159–5172.

Shepherd, T. G. (2003), Large-scale atmospheric dynamics for atmospheric chemists, *Chem. Rev.*, *103*(12), 4509–4532, doi:10.1021/cr020511z.

Stanford, J. L., and J. R. Ziemke (1991), CH_4 and N_2O photochemical lifetimes in the upper stratosphere: In situ estimates using SAMS data, *Geophys. Res. Lett.*, *18*, 677–680.

Sugita, T., et al. (2002), Validation of ozone measurements from the Improved Limb Atmospheric Spectrometer (ILAS), *J. Geophys. Res.*, *107*(D24), 8212, doi:10.1029/2001JD000602.

Sugita, T., et al. (2006), Ozone profiles in the high-latitude stratosphere and lower mesosphere measured by the Improved Limb Atmospheric Spectrometer (ILAS)-II: Comparison with other satellite sensors and ozonesondes, *J. Geophys. Res.*, *111*, D11S02, doi:10.1029/2005JD006439.

Terao, Y., Y. Sasano, H. Nakajima, H. Tanaka, and T. Yasunari (2002), Stratospheric ozone loss in the 1996/1997 Arctic winter: Evaluation based on multiple trajectory analysis for double-sounded air parcels by ILAS, *J. Geophys. Res.*, *107*(D24), 8210, doi:10.1029/2001JD000615.

Tilmes, S., R. Müller, J.-U. Grooß, M. Höpfner, G. C. Toon, and J. M. Russell (2003a), Very early chlorine activation and ozone loss in the Arctic winter 2002–2003, *Geophys. Res. Lett.*, *30*(23), 2201, doi:10.1029/2003GL018079.

Tilmes, S., R. Müller, J.-U. Grooß, D. S. McKenna, J. M. Russell, and Y. Sasano (2003b), Calculation of chemical ozone loss in the Arctic winter 1996–1997 using ozone-tracer correlations: Comparison of Improved Limb Atmospheric Spectrometer (ILAS) and Halogen Occultation (HALOE) results, *J. Geophys. Res.*, *108*(D2), 4045, doi:10.1029/2002JD002213.

Tilmes, S., R. Müller, J.-U. Grooß, and J. M. Russell (2004), Ozone loss and chlorine activation in the Arctic winters 1991–2003 derived with the tracer-tracer correlations, *Atmos. Chem. Phys.*, *4*, 2181–2213.

Tilmes, S., R. Müller, J.-U. Grooß, R. Spang, H. Nakajima, and Y. Sasano (2006), Chemical ozone loss and related processes in the Antarctic winter 2003 based on Improved Limb Atmospheric Spectrometer (ILAS)-II observations, *J. Geophys. Res.*, *111*, D11S12, doi:10.1029/2005JD006260.

Yokota, T., et al. (2002), Improved Limb Atmospheric Spectrometer (ILAS) data retrieval algorithm for version 5.20 gas profile products, *J. Geophys. Res.*, *107*(D24), 8216, doi:10.1029/2001JD000628.

F. Khosrawi, Department of Applied Environmental Science/Department of Meteorology, Stockholm University, SE-10691 Stockholm, Sweden. (farahnaz.khosrawi@itm.su.se)

R. Müller, ICG-I: Stratosphere, Forschungszentrum Jülich, D-52425 Jülich, Germany. (ro.mueller@fz-juelich.de)

H. Nakajima, Ozone Layer Research Project, National Institute for Environmental Studies, 16-2 Onogawa, Tsukuba, Ibaraki 305-8506, Japan. (hide@nies.go.jp)

M. H. Proffitt, Proffitt Instruments Inc., 7502 Valburn Drive, Austin, TX 78731, USA. (proffitt@uolsinectis.com.ar)